Annals of Biomedical Engineering, Vol. 38, No. 12, December 2010 *(© 2010)* pp. 3744–3755
DOI: 10.1007/s10439-010-0113-4

On Non-Invasive Measurement of Gastric Motility from Finger Photoplethysmographic Signal

S. Mohamed Yacin,[1] M. Manivannan,[1] and V. Srinivasa Chakravarthy[2]

[1]Touch Lab, Department of Applied Mechanics, Indian Institute of Technology Madras, Chennai 600036, Tamilnadu, India; and [2]Computational Neuroscience Lab, Department of Biotechnology, Indian Institute of Technology Madras, Chennai 600036, Tamilnadu, India

(Received 18 January 2010; accepted 22 June 2010; published online 8 July 2010)

Associate Editor Leonidas D. Iasemidis oversaw the review of this article.

Abstract—This article investigates the possibility of extracting gastric motility (GM) information from finger photoplethysmographic (PPG) signals non-invasively. Now-a-days measuring GM is a challenging task because of invasive and complicated clinical procedures involved. It is well-known that the PPG signal acquired from finger consists of information related to heart rate and respiratory rate. This thread is taken further and effort has been put here to find whether it is possible to extract GM information from finger PPG in an easier way and without discomfort to the patients. Finger PPG and GM (measured using Electrogastrogram, EGG) signals were acquired simultaneously at the rate of 100 Hz from eight healthy subjects for 30 min duration in fasting and postprandial states. In this study, we process the finger PPG signal and extract a slow wave that is analogous to actual EGG signal. To this end, we chose two advanced signal processing approaches: first, we perform discrete wavelet transform (DWT) to separate the different components, since PPG and EGG signals are non-stationary in nature. Second, in the frequency domain, we perform cross-spectral and coherence analysis using autoregressive (AR) spectral estimation method in order to compare the spectral details of recorded PPG and EGG signals. In DWT, a lower frequency oscillation (≈0.05 Hz) called slow wave was extracted from PPG signal which looks similar to the slow wave of GM in both shape and frequency in the range (0–0.1953) Hz. Comparison of these two slow wave signals was done by normalized cross-correlation technique. Cross-correlation values are found to be high (range 0.68–0.82, SD 0.12, $R = 1.0$ indicates exact agreement, $p < 0.05$) for all subjects and there is no significant difference in cross-correlation between fasting and postprandial states. The coherence analysis results demonstrate that a moderate coherence (range 0.5–0.7, SD 0.13, $p < 0.05$) exists between EGG and PPG signal in the "slow wave" frequency band, without any significant change in the level of coherence in postprandial state. These results indicate that finger PPG signal contains GM-related information. The findings are sufficiently encouraging to motivate further exploration of finger PPG as a non-invasive source of GM-related information.

Keywords—AR spectral estimation, Cross-correlation, Discrete wavelet transform, Electrogastrography, Enteric nervous system, Gastric myoelectric activity, Magnitude squared coherence, Slow wave.

INTRODUCTION

Photoplethysmography (PPG) is a well-known, simple and non-invasive technique to monitor physiological parameters in intensive care units and medical research laboratories.[3,13] It measures volumetric changes in blood vessels that mainly occur in arteries and arterioles.[4,27,48,51] PPG method gained popularity because it is easy to acquire, and contains numerous clinical parameters such as heart rate, respiratory-induced intensity variations (RIIV),[29,30,46] and oxygen saturation levels in blood (called as pulse oximeter).[3,58,61] In finger PPG, an infrared beam traveling through the fingertip is absorbed by pulsatile arterial blood, venous blood, and other absorbing tissues such as skin pigmentation and bone, and the transmitted or reflected beam is detected by a photo detector.[3,13,27,31] PPG signal mainly consists of two components, pulsatile component due to the arterial blood (AC component) and the stationary part (DC component) due to absorbance of venous blood, the fixed quantity of arterial blood, and other stationary components like skin pigmentation.[27,29,30] PPG signal provides information about the cardiovascular dynamics and also reflects activities of the sympathetic and vagus

Address correspondence to M. Manivannan, Touch Lab, Department of Applied Mechanics, Indian Institute of Technology Madras, Chennai 600036, Tamilnadu, India. Electronic mail: s_yacin@yahoo.co.in, mani@iitm.ac.in, schakra@ ee.iitm.ac.in

nerves.[48] Therefore, PPG analysis seems to be of great significance in a variety of clinical applications, particularly in evaluation of the status of cardiovascular system. It has been estimated that the PPG signal is composite in nature and has five different frequency components in the interval (0.007–1.5) Hz.[35,56] These frequency components may be related to heart rate, respiration, blood pressure control, thermoregulation, central baroreflex activity, vasomotoric rhythms, autonomous nervous system (ANS), and heart-synchronous pulse waveform. The origins of these PPG signal components are not fully understood because of the highly complicated nature of the circulatory system, especially in the skin level microcirculation where regulatory processes are of both central and local origin.[28,32,36,47]

Our hypothesis is that since human circulatory system constitutes many interacting subsystems like cerebral circulation, pulmonary circulation, splanchnic circulation, etc., rhythm changes in one subsystem could possibly manifest in the activities of the other subsystems. Therefore, hemodynamics in any separate subsystem is influenced by hemodynamic interactions throughout the whole system because it is a closed-loop system.[39] There are experimental evidences that confirms the existence of a functional relationship between gastrointestinal (GI) system and cardiovascular function.[39,52] Starting from this perspective, the present work investigates the possibility of extracting GI-system-related information from finger PPG signal. A schematic representation of human circulatory system with major subsystems is shown in Fig. 1.

Finding the activity of internal visceral organs such as stomach, kidney by non-invasive PPG is a clinically challenging task. A quantitative report of abdominal PPG signals at red and infrared wavelengths have been investigated invasively and showed that the PPG can also be used to measure blood volume change in abdominal organs.[37] Intestinal ischemia and GI perfusion pressure was also experimentally measured in canine model using PPG.[5,21] It was also stated that the peripheral blood flow dynamics changes due to change in blood supply to the smooth muscles of the stomach during digestion.[20,57] Wavelet analysis of blood flow signal measured by PPG and laser Doppler flow meter was studied.[35,56] It was shown that the rhythmic oscillation in the frequency range (0.04–0.1) Hz may be due to myogenic activity of smooth muscles or neurogenic activity.[56] This observation supports our hypothesis that GM-related information may also be present in finger PPG and it can be extracted using appropriate signal processing techniques.

Human stomach is an enlarged, muscular sac-like organ of the alimentary canal and the principal organ of digestion. Its motor functions include accommodation of ingested food, grinding food chunks, mixing of secretory gastric juice into food particles, and delivery of food chyme into the duodenum.[6] In order to accomplish the whole digestive process of the stomach, from mixing, stirring, agitating, propelling and to emptying, a spatiotemporal activation pattern is formed in the gut walls.[6,23] This pattern is called gastric myoelectrical activity (GMA) which originates from the pacemaker located in proximal body of the stomach and the effect of it results in gastric motility (GM). It manifests the continuously rhythmic change in the membrane potential, which propagates to the distal antrum with a regular frequency of about three cycles per minute (cpm, 0.05 Hz).[15] Normal GM was defined as a frequency between 2 and 4 cpm. It is believed that the interstitial cells of Cajal (ICC) of enteric nervous system (ENS) generate the rhythmic depolarizations of the gastric slow wave. Additional depolarizations provided by neurohumoral stimulation are the triggers for phasic gastric contractions which follow the spread of the electrical slow waves and are peristaltic. Thus, gastric electrical slow waves control the maximal frequency and the direction of contractions in the distal stomach.[49] Recording of this GM is called electrogastrography (EGG) and it can be measured non-invasively by positioning surface electrodes

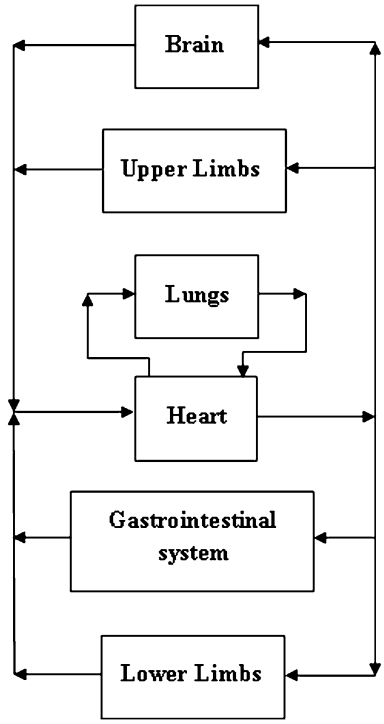

FIGURE 1. Schematic of the human circulatory system highlighting the connection of gastrointestinal system to the peripheral circulatory system.

over the abdominal skin. EGG measurement shows with reasonable accuracy a slow wave pattern corresponding to the overall GM function.[49,55]

The central theme of this article is to investigate the existence of gastric rhythms in finger PPG. To explain this idea, let us use a slightly abstract schematic in the form of a simple electric analog (Fig. 2). Let the AC source, oscillating at a frequency of 72 beats per min (ω_h), shown in the circuit of Fig. 2, represent the human heart. Let the gut be described as a time-varying resistor ($R_g(t)$) which varies at the frequency of 3 cpm (ω_g) and arterial resistance is denoted as R_a. The resistor (R_{ra}) denotes the radial artery and current, I_{ra}, in this branch represents the finger PPG signal that is measured.

Note that for this simple resistive circuit, I_{ra}, turns out to be:

$$I_{ra}(t) = \frac{V(t)R_g(t)}{R_{ra}R_g(t) + R_a(R_{ra} + R_g(t))} \quad (1)$$

Note that I_{ra} reflects oscillations in gut resistance $R_g(t)$ also. We concede that the above schematic cannot obviously serve as a "proof" of existence of gastric rhythms in finger PPG. At its best it only serves to express the hypothesis of "the presence of gastric rhythms in finger PPG" in a concrete fashion.

The relationship between PPG signals and cardiopulmonary system parameters has been found widely in the literature. However, very few reports have been examined concerning the relationship between PPG and EGG signals. The objective of the present study is to investigate whether it is possible to extract GM-related information from PPG signal, considering that the gut may be treated as a time-varying load located on one of the branches of the cardiovascular network. The PPG and EGG are non-stationary signals in nature by means of its frequency, magnitude, and shape of the wave. Any signal processing performed on these signals must therefore be suitable for non-stationary signals, which rules out many traditional filtering techniques. Discrete wavelet transform (DWT) is an advanced signal processing method designed for non-stationary signals.[2,17,18] It incorporates the concept of scale into the transform, which gives better time–frequency resolution: a compressed wavelet is used for analyzing high-frequency details and a dilated wavelet for detecting lower frequency underlying trends.[16] The DWT method is utilized for multi-level decomposition of PPG and EGG signals of eight healthy subjects in fasting and postprandial states. Cross-correlation is a well-established approach for comparing signals.[34,43,44] It has wide applications including audio-signal processing and image processing. In the field of PPG, cross-correlation method has been used to assess the similarity of PPG signals acquired from ears, thumbs, and toes.[4] To our knowledge, cross-correlation has never been used to compare PPG and EGG signals, with the purpose of looking for the presence of the latter in the former.

Coherence analysis is another important signal processing technique, which reveals the correlation between two signals at specific frequencies.[11] This analysis has been applied in the past for comparing heart sounds that are simultaneously recorded from aortic area, pulmonary area, mitral area, and tricuspid area.[22,24,25] The same method was used to compare finger PPG and respiratory signals using autoregressive (AR) model.[41] However, coherence analysis between raw PPG and EGG signals has not been explored before. This article examines the presence of GM information in finger PPG signal and analyses the level of coherence between finger PPG and EGG signals using magnitude squared coherence (MSC) technique. The results of this study verify that there exists a corresponding GM component in spectrum of raw PPG signal acquired from finger area. The results may provide an attractive approach to acquire the GM information from PPG without discomfort to the patients.

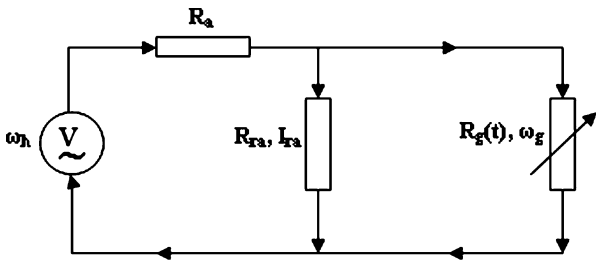

FIGURE 2. An abstract model of the human circulatory system (*V* heart as the voltage source, R_a arterial tree, R_{ra} radial artery, $R_g(t)$ gut as the time-varying resistor).

MATERIALS AND METHODS

Subjects

This study was executed with eight healthy non-habitual smoking and non-sports male subjects without disorders and symptoms of GI, cardiovascular or any other diseases. The volunteers were recruited from the student community of our institute. Subjects mean age was 22.0 ± 2.7 (SD) years in the range of 20 and 28 years and the mean body mass index (BMI) was 22.3 ± 1.7 (SD) (range 19.7–25.3). This study was approved by our institute ethics committee and all the subjects were given informed consent before data recording.

Data Acquisition and Hardware

We acquired the PPG signal from the left hand index finger using a reflection type infrared sensor (SS4LA, Biopac Systems, Inc, USA). Volunteers were informed to observe silence and to keep relatively still during data recording time to minimize motion artifacts. EGG signals are measured by Ag–AgCl electrodes (SS2L, Biopac Systems, Inc, USA) placed over the abdominal surface. The skin area in the abdominal surface was cleaned with sandy skin prepping paste to reduce the skin resistance and to minimize skin electrode motion artifacts. Three disposable surface electrodes filled with electrode jelly were placed over on the abdominal skin. Out of three, two active electrodes were placed below the left costal margin and in between the xyphoid process and umbilicus. The third one considered as reference electrode was positioned in the right upper quadrant. Real time recording unit MP 35 (Biopac Systems Inc, USA) is used here for data acquisition.

After allowing the subject to rest in a supine position for 15 min in order to maintain a stable heart beat and respiration, PPG and EGG signals were recorded in the following manner. Fasting data were recorded for 30 min in the supine position after 5 h of fasting. Then the subjects were allowed to take a meal (comprised of limited rice, fruit slices and one cup of water) in a sitting position and then again assume supine position. Data were also collected in postprandial condition immediately after meal for more than 30 min. During data recording procedure, all the subjects were asked to maintain normal and stable breathing rate (12–18 cycles per minute = 0.2–0.3 Hz) and to the extent possible, kept quiet and remain in the same position. Temperature was regulated at 25 ± 1 °C in the data recording room. During acquisition the gain was adjusted to 2000 for finger PPG signal and it was 5000 for EGG signal. Both the finger PPG and EGG signals were acquired at the sampling rate of 100 samples per second. After raw data acquisition, the signals are detrended and then processed by 0.01 Hz high-pass filter in order to remove the baseline wandering. A second order Butterworth low-pass filter with a cutoff frequency of 40 Hz was selected for finger PPG and 0.4 Hz was selected for EGG. Major movement artifacts, if any, are found by direct visual inspection of the waveform. Abnormally large positive or negative peaks in the tracing were identified by direct visual analysis and treated as movement artifact; the same was removed using a separate program before applying the signal processing techniques. This program sets threshold amplitude and removes the data points whenever it crosses the threshold value. For example, if the signal varies between ±1 V, a threshold limit is set with ±2 V. If the signal crosses threshold, it will be treated as artifact and the same will be removed. A portion of the signals recorded from the same subject during fasting and postprandial states are shown in Figs. 3 and 4. A dedicated personal computer (PC) was used for storage, display and analysis of the acquired finger PPG and EGG data. All experimental data presented in this article were expressed as mean ± standard deviation, and p values <0.05 were considered to be statistically significant.

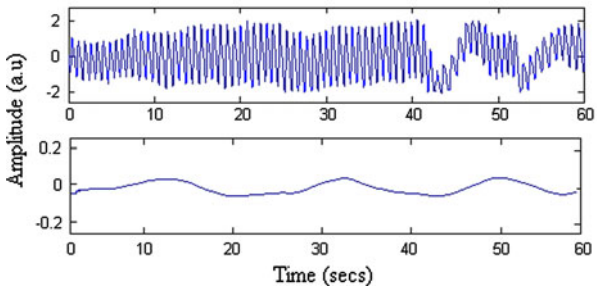

FIGURE 3. Finger PPG and EGG signals recorded in fasting state.

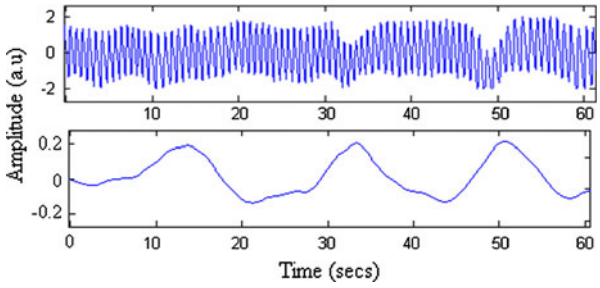

FIGURE 4. Finger PPG and EGG signals recorded in postprandial state.

Discrete Wavelet Transform

The wavelet analysis is expressed in terms of *approximations and details*. The approximations are defined as the high-scale, low-frequency contents and the details are defined as the low-scale, high-frequency contents present in the signal. DWT analyzes the signal at different frequency bands with different resolutions by decomposing the signal into coarse approximation and detail coefficients as shown in Fig. 5. These coefficients represent different frequency subbands. All wavelet transforms can be specified in terms of a low-pass filter with impulse response h, which satisfies the standard quadrature mirror filter condition:

$$H(z)H(z^{-1}) + H(-z)H(-z^{-1}) = 1, \qquad (2)$$

where $H(z)$ denotes the z-transform of the filter h. Its complementary high-pass filter can be defined as

$$G(z) = zH(-z^{-1}) \qquad (3)$$

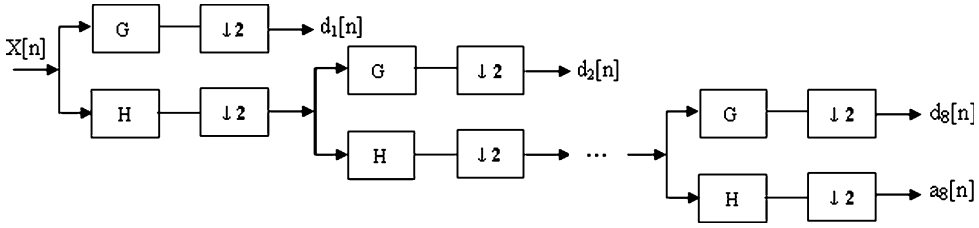

FIGURE 5. Discrete wavelet transform multi-level decomposing process.

A sequence of filters with increasing length (indexed by i) can be obtained.

$$H_{i+1}(z) = H\left(z^{2^i}\right) H_i(z), \tag{4}$$

$$G_{i+1}(z) = G\left(z^{2^i}\right) H_i(z), \quad i = 0, \ldots I-1 \tag{5}$$

with the initial condition $H_0(z) = 1$. It is expressed as a two-scale relation in time domain

$$h_{i+1}(k) = [h]_{\uparrow 2^i} * h_i(k), \tag{6}$$

$$g_{i+1}(k) = [g]_{\uparrow 2^i} * h_i(k), \tag{7}$$

where the subscript $[\cdot \leftarrow]^{\uparrow m}$ indicates the up-sampling by a factor of m, and k is uniformly sampled discrete time index. DWT employs two sets of functions, called scaling functions and wavelet functions, which are associated with low-pass and high-pass filters, respectively. The normalized wavelet and scale basis functions $\varphi_{i,l}(k)$, $\psi_{i,l}(k)$ can be defined as

$$\varphi_{i,l}(k) = 2^{i/2} h_i(k - 2^i l), \tag{8}$$

$$\psi_{i,l}(k) = 2^{i/2} g_i(k - 2^i l), \tag{9}$$

where factor $2^{i/2}$ is an inner product normalization, and i and l are the scale parameter and the translation parameter, respectively. The DWT decomposition can be described as

$$s_i(l) = x(k) * \varphi_{i,l}(k), \tag{10}$$

$$d_i(l) = x(k) * \psi_{i,l}(k), \tag{11}$$

where $s_i(l)$ and $d_i(l)$ are the approximation coefficients and the detail coefficients at resolution i, respectively.[16–18]

At each level, high-pass filter produces details information, $d[n]$, while the low-pass filter associated with scaling function produces coarse approximations, $a[n]$. At each decomposition level, the half band filters produce signals spanning only half the frequency band. This doubles the frequency resolution as the uncertainty in frequency is reduced by half. In accordance with Nyquist's rule if the original signal has highest frequency of ω, which requires a sampling frequency of 2ω radians/s, then it now has a highest frequency of $\omega/2$ radians/s. It can now be sampled at a frequency of ω radians thus discarding half the samples with no loss of information. This subsampling by two halves the time resolution, as the entire signal is now represented by only half the number of samples. Thus, while subsampling the frequency band of low-pass filter becomes half of the previous band which doubles the scale. With this approach, the time resolution becomes arbitrarily good at high frequencies, while the frequency resolution becomes arbitrarily good at low frequencies.[33,56]

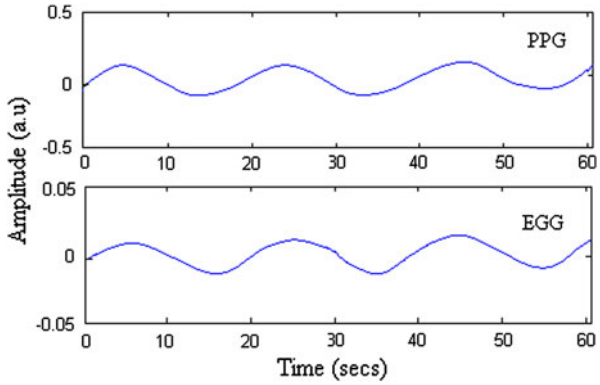

FIGURE 6. Slow waves reconstructed from eighth level approximation matrices in fasting state.

In the present study, signals were decomposed using Daubechies mother wavelet of order ("db3") because of its suitability for biomedical signals like PPG and EGG.[17,33,56,60] Eighth level approximation coefficients matrices, which approximately correspond to the frequency range (0–0.1953) Hz are taken for further analysis.

A signal, called *slow wave* is reconstructed from eighth level approximation coefficients matrices of finger PPG and EGG signals and are shown in Figs. 6 and 7, respectively. The horizontal axis is the time in seconds, whereas the vertical axis is the amplitude expressed in arbitrary units.

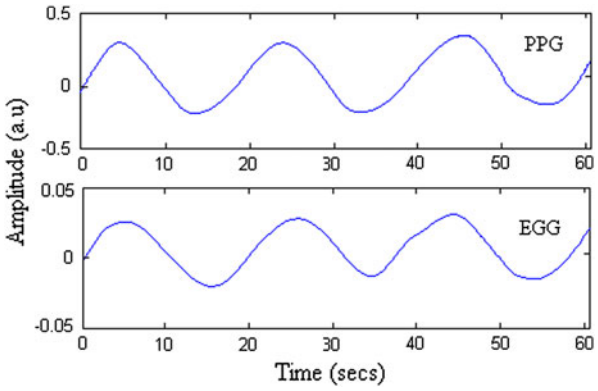

FIGURE 7. Slow waves reconstructed from eighth level approximation matrices in postprandial state.

Cross-Correlation Analysis

Cross-correlation between two time series measures the degree of similarity between the signals.[43,50,54] It provides a quantitative measure of the relatedness of two signals, usually from different recording sites, as they are progressively shifted in time with respect to each other. Consider that the two series x_i and y_i are the *slow waves* of PPG and EGG, respectively, where N is the number of samples and $i = 0,1,2,\ldots,N-1$. The normalized cross-correlation function with zero time lag is calculated as

$$R = \frac{\sum x_i y_i}{(\sum x_i^2)^{1/2}(\sum y_i^2)^{1/2}} \tag{12}$$

Here, the two series x_i and y_i are zero mean signals. Equation (12) calculates the similarity in shape between two curves as a scalar between -1 and 1, with 1 indicating perfect correlation, -1 indicating perfect correlation with 180° phase shift and zero indicating no correlation. Cross-correlation results do not change while changing the amplitude of the curve only when there is no change in its shape. In this work, cross-correlation analysis was done to compare slow waves of finger PPG and EGG in fasting and postprandial conditions.

Autoregressive Model Coherence Analysis

A pair of signals can be compared in time domain using the cross-correlation and correlation coefficients; cross-spectrum and coherence function can be used in the frequency-domain analysis. While the time-domain analysis provides a measure of similarity as a function of time lag, the frequency-domain analysis provides a measure of similarity as a function of frequency.[8,11,26] Since our objective here is the frequency-domain analysis of finger PPG and EGG signals, we choose the cross-spectral estimation method, for comparison.

For a two-channel random process consisting of two data vectors $x(n)$ and $y(n)$, the Hermitian matrix $C(f)$, associated with the auto- and cross-spectrum of the signal pair is called the "coherence matrix" and is used to measure the similarity between the two random process as a function of frequency

$$C(f) = \begin{vmatrix} G_{xx}(f) & G_{xy}(f) \\ G_{yx}(f) & G_{yy}(f) \end{vmatrix}, \tag{13}$$

where $G_{xx}(f)$ and $G_{yy}(f)$ are the auto-spectrums, $G_{xy}(f)$ and $G_{yx}(f)$ are the cross-spectrums and the expression

$$\Phi(f) = \frac{G_{xy}(f)}{\sqrt{G_{xx}(f)}\sqrt{G_{yy}(f)}} \tag{14}$$

is termed as the "coherence function" which can also be defined in terms of the MSC and the coherence phase spectrum:

$$\mathrm{MSC}(f) = |\Phi(f)|^2 \tag{15}$$

$$\theta(f) = \angle\Phi(f) \tag{16}$$

The MSC lies between 0 (if there is no coherence between the two frequencies) and 1 (if there is a perfect coherence between the frequencies). Thus, the MSC may be used to measure the similarity between a pair of signals as a function of frequency, providing a suitable tool for the purpose of the current study.[25,41] The coherent phase, on the other hand, represents the phase lag or lead of one channel with respect to the other channel as a function of frequency. This allows studying the relationship between finger PPG and EGG, particularly when the gut is in a state of increased motility.

The classical FFT-based methods, such as the Welch method,[34,43] for estimating the coherence function suffer from an inherent bias toward an over-estimation of the MSC function.[8,9,11] This problem is more pronounced if the averaging process involved in these methods is ignored. For signals of short duration, such as PPG, it is only possible to have a limited number of segments for averaging. Therefore, a bias in the MSC function is inevitable which results in an overestimation of the degree of coherence between the two channels. As a result, the classical methods for multichannel spectral estimation are not capable of providing an efficient tool for the purpose of this study. In contrast, multichannel model-based spectral estimation methods are known to be capable of estimating the coherence function without introducing bias into the resultant MSC function.[11,34,43,59]

The multichannel AR process of order p is defined as the vector recursion

$$X(n) = -\sum_{k=1}^{p} A(k)X(n-k) + u(k), \qquad (17)$$

where $X(n)$ denote the vector of samples from multichannel AR process at sample index n, $A(k)$ is the AR parameter matrix (for each order), and $u(k)$ represents the input driving noise process. After estimating the AR parameters, two-channel coherence matrix is calculated by multiplying the squared magnitude of the transfer function of the two-channel filter[24] and the covariance matrix of the input noise, and then scaling the result with the sampling interval, T

$$P_{\mathrm{AR}}(f) = T[A(f)]^{-1}P_{\mathrm{c}}[A(f)]^{-H} \qquad (18)$$

in which

$$A(f) = I + \sum_{k=1}^{p} A(k)e^{-j2\pi fkT}, \qquad (19)$$

where H denotes the Hermitian transpose of the inverse, P_{c} is the covariance matrix of the input noise process, and I denotes the identity matrix. The two-channel AR parameters and the covariance matrix of the input driving noise are estimated by the Vieira-Morf algorithm through the minimization of the geometric mean of the forward and backward prediction errors.[25] All these signal processing techniques were done in MATLAB 7.0 release 14.1 (The MathWorks co. MATLAB® version 7.2).

RESULTS AND DISCUSSION

There have been many experimental studies on PPG low-frequency oscillations and extracting information about cardiopulmonary parameters with various degrees of accuracy. However, very little attention has been given to the possibility of extracting GM data from finger PPG. In the present study, we used DWT for feature extraction because of its high-frequency resolution at low-frequency ranges (high scales). The DWT coefficients from the eighth approximation level, which corresponds to the frequency of approximately (0–0.1953) Hz, were extracted from both finger PPG and EGG separately and cross-correlation analysis was performed. A filtered EGG slow wave was reconstructed from DWT coefficients matrices of eighth approximation level because most of the artifacts are removed by the high-pass filters (details). In finger PPG DWT decomposition, the expected high-frequency components such as heart rate (≈1 Hz) and respiratory rate (≈0.3 Hz) information were also removed using high-pass filters (details) and the slow wave was taken for analysis which are shown in Fig. 6 for fasting state and Fig. 7 for postprandial state for the same subject. The difference in amplitudes of slow waves of finger PPG and EGG arises from the difference in the original signal strengths (volts for finger PPG and microvolts for EGG) at the time of acquisition. Though only the results from one subject are displayed in this article, similar results are derived from other subjects. The frequency of slow waves reconstructed from DWT coefficients of EGG and finger PPG are shown in Table 1 for both fasting state and postprandial states. Here, the 30 min data was split into three 10 min long segments, and the three dominant frequencies were calculated for these segments for all the subjects. This is to ensure that the dominant signal frequency does not change appreciably during the 30 min recording time. Average values of mean power were calculated from eighth level DWT coefficients of EGG and finger PPG slow waves for the 30 min data. Student's t test was performed to compare the mean power of the wavelet coefficients in two different states; power in postprandial state is higher than that in fasting state in statistical terms

TABLE 1. Comparison of slow wave frequencies of EGG and PPG calculated from DWT eighth level decomposition level in fasting and postprandial state.

	EGG slow waves signal frequency in eighth DWT decomposition level (Hz)		PPG slow waves signal frequency in eighth DWT decomposition level (Hz)	
Subject number	Fasting state	Postprandial state	Fasting state	Postprandial state
1	0.051 ± 0.002	0.052 ± 0.003	0.049 ± 0.002	0.051 ± 0.001
2	0.052 ± 0.004	0.055 ± 0.002	0.049 ± 0.003	0.052 ± 0.002
3	0.049 ± 0.003	0.051 ± 0.005	0.057 ± 0.006	0.055 ± 0.004
4	0.052 ± 0.004	0.053 ± 0.005	0.052 ± 0.003	0.053 ± 0.002
5	0.049 ± 0.003	0.051 ± 0.004	0.051 ± 0.004	0.055 ± 0.005
6	0.051 ± 0.001	0.052 ± 0.001	0.049 ± 0.005	0.051 ± 0.003
7	0.051 ± 0.003	0.052 ± 0.005	0.049 ± 0.003	0.051 ± 0.005
8	0.052 ± 0.005	0.055 ± 0.003	0.056 ± 0.004	0.060 ± 0.003

Values are expressed in mean ± standard deviation.

TABLE 2. Comparison of average mean power of EGG and PPG slow waves calculated from DWT eighth level decomposition level in fasting and postprandial state.

	EGG slow waves mean power of eighth decomposition level DWT coefficients (mV^2/Hz)		PPG slow waves mean power of eighth decomposition level DWT coefficients (mV^2/Hz)	
Subject number	Fasting state	Postprandial state	Fasting state	Postprandial state
1	29.32 ± 2.51	58.26 ± 5.34	310.21 ± 17.21	520.62 ± 25.42
2	32.41 ± 2.32	59.42 ± 6.56	320.38 ± 16.22	525.42 ± 23.64
3	45.21 ± 2.65	83.81 ± 8.24	410.21 ± 17.64	740.17 ± 28.23
4	29.24 ± 2.82	58.21 ± 3.48	385.25 ± 14.33	640.22 ± 24.52
5	32.23 ± 2.32	62.14 ± 3.48	330.36 ± 21.32	565.26 ± 32.62
6	27.51 ± 2.23	62.12 ± 2.82	310.20 ± 21.32	526.32 ± 24.24
7	29.12 ± 3.85	64.18 ± 6.32	374.24 ± 19.48	556.53 ± 27.52
8	35.62 ± 4.32	65.78 ± 7.23	366.54 ± 25.52	605.26 ± 28.42

Values are expressed in mean ± standard deviation.

(p values <0.05). Average mean power values of all the subjects from finger PPG and EGG slow waves are shown in Table 2.

Though some studies regard PPG signal variability as a manifestation of ANS activity in general,[48] the influence of ENS, which is considered as a part of ANS, on finger PPG is not well explored. GMA amplitude is higher in the postprandial state and was observed as increase in EGG signal mean power (square of the amplitude per Hz), which is well-established and proved.[49] The increase in EGG slow wave power from fasting to postprandial state was found in all the subjects (see Table 2) with a correlation of $0.91(p < 0.05)$. This may be due to the increase in splanchnic blood supply[20] to the gastric muscle for strong muscle contraction during digestion and absorption of nutrients[57] and decrease in blood supply to the extremities which is observed as increase in power of finger PPG slow waves (see Table 2). The change in frequency and power of the finger PPG slow wave signals are proportional to the EGG frequency and power. Also the increase in finger PPG slow wave power from fasting to postprandial state was found in all the subjects with a correlation of $0.89(p < 0.05)$. The rhythm corresponding to these large blood volume changes in the gut, seems to manifest itself in the finger PPG. Because the human cardiovascular system is a closed-loop system, hemodynamics in any separate segment(gut) is determined by hemodynamic interactions throughout the whole system.[39] In this preliminary work, it is revealed that there is a significant correlation between finger PPG and EGG (Slow waves) in healthy humans.

Cross-correlation analysis performed between slow waves of EGG and finger PPG yielded promising results with R-value >0.7 (95% confidence level) for most of the subjects (see Table 3). This indicated that the slow wave patterns of finger PPG and EGG for an individual subject are consistent in different conditions (fasting/postprandial). This also suggests that finger PPG signal may have information about GMA because of physiological nature of the system and needs to be confirmed by further research. DWT should therefore be a useful method for extracting GMA for a given subject in different gastric-related conditions, such as fasting and postprandial states. While this method provides a new and alternative method for the extraction of GMA, it should be noted that the accuracy of this method is associated with the finger PPG recording and selection of the mother wavelet.[7,10] Therefore, during the recording, every effort should be made to assure the highest possible signal-to-noise ratio, appropriate placement of finger PPG sensor, minimization or elimination of motion artifacts and constant environmental conditions.

TABLE 3. Comparison of cross-correlation results (R-values) of slow waves of EGG and PPG after DWT.

	Normalized cross-correlation (R) values	
Subject number	R-value in fasting state	R-value in postprandial state
1	0.75 ± 0.02	0.77 ± 0.05
2	0.72 ± 0.06	0.74 ± 0.09
3	0.72 ± 0.16	0.73 ± 0.11
4	0.81 ± 0.08	0.82 ± 0.03
5	0.72 ± 0.03	0.73 ± 0.11
6	0.68 ± 0.08	0.69 ± 0.13
7	0.73 ± 0.05	0.75 ± 0.15
8	0.73 ± 0.06	0.76 ± 0.02

Values are expressed in mean ± standard deviation.

Coherence between the recorded finger PPG and EGG signals under fasting/postprandial conditions from all the subjects was also analyzed to evaluate their relationships in frequency domain. In finger PPG signal, it is expected to have mostly three predominant frequencies. They are due to the cardiac frequency,

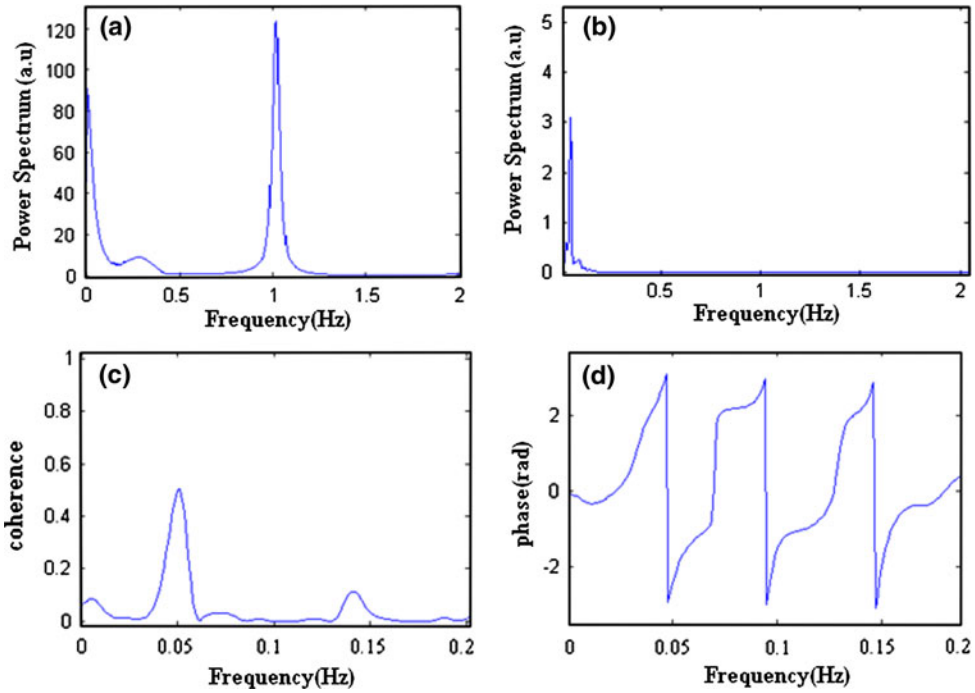

FIGURE 8. Coherence analysis in fasting state (a) PSD of finger PPG signal, (b) PSD of EGG signal, (c) MSC, and (d) coherence phase.

breathing frequency and another due to the lower frequency that is often present in the recorded signal. Using this as *a priori* knowledge of the signal, a model order of 50 was considered here based on literature.[1,43,50] Since AR model is a stable and all-pole filter, the magnitude of the poles lie inside the unit circle.[42,53] The existence of coherent peak can be determined by checking whether the corresponding pole inside the unit circle is prominent or not. The prominence of a pole inside the unit circle is determined by its magnitude. The pole with maximum magnitude inside the unit circle is considered as the prominent pole.[12,19,38] Figures 8c and 8d show the coherence analysis results of the subject in the fasting state. As seen in Fig. 8c, MSC is >0.5 near 0.05 Hz (the GMA frequency). Also, the coherence phase is smaller than zero (Fig. 8d), which means that the GMA-induced changes in finger PPG signal lags the EGG signal. It can also be noted that there is a corresponding lower frequency component near the EGG frequency in the PSD of finger PPG signal, as depicted in Fig. 8a. The results in the postprandial condition for the same subject are demonstrated in Fig. 9. The MSC depicts that coherence level slightly increases between EGG and finger PPG signal (Fig. 9c) in the postprandial state, but without change in time delay induced by GMA, as shown in Fig. 9d. This increase in MSC may be due to higher rhythmic waves of EGG which means very strong rhythmic gastric muscle contraction in the postprandial state.[14] The MSC values are in between 0.5 and 0.7, which shows that there exists a moderate coherence between EGG and finger PPG signals around the frequency of interest. If the Fourier-based techniques were applied in the analysis, the GMA-related component will not be as obvious as depicted in this research.[16,33,40,45] Though only the results from one subject are depicted in this article, similar results are derived for almost all subjects. Coherence analysis between raw finger PPG and respiratory movement showed that the level of coherence was more than 0.9.[41] However, in our study the observed level of coherence between finger PPG and EGG was between 0.5 and 0.7. The main reason for this moderate coherence may be due to the nature of interaction between the two subsystems; heart rhythm, the source of PPG and respiratory rates are more interrelated than GM with heart rhythm and also rhythms from baroreflex and vasomotor sources overlaps with the 0.05 Hz frequency range. It may be possible to acquire the GMA information from finger PPG signal by single-channel AR method with the consideration of poles in a physiologically plausible GMA frequency range.[12,19]

CONCLUSION

Feature extraction of clinically important parameters from PPG is gaining popularity because of its low cost, non-invasiveness, and ease of acquisition.

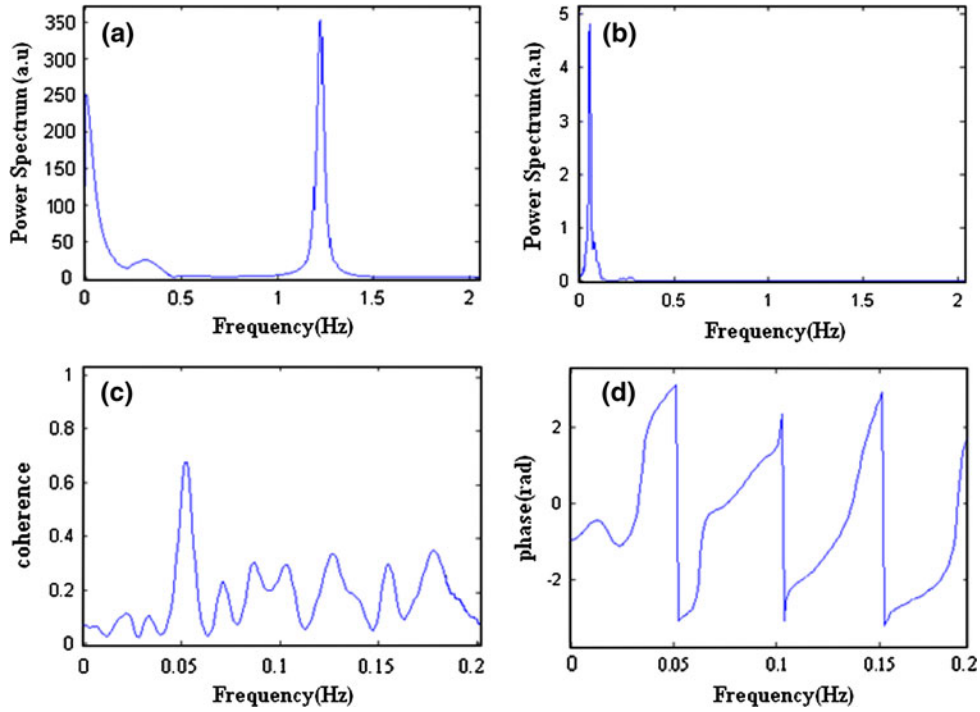

FIGURE 9. Coherence analysis in postprandial state (a) PSD of finger PPG signal, (b) PSD of EGG signal, (c) MSC, and (d) coherence phase.

Estimation of GMA from EGG is difficult because of its poor signal-to-noise ratio and discomfort to the patients. In this study, two advanced signal processing techniques have been used to extract GMA-related information from finger PPG signal. Using DWT a slow wave is extracted from finger PPG by decomposing the signal into details and approximation coefficients. The use of DWT with cross-correlation analysis allowed a closer investigation of the lower frequency oscillations of PPG and its intermittent behavior during fasting and postprandial conditions. This study indicates that there is a good correlation (0.68 and 0.82) between the slow waves of finger PPG with EGG. While these correlation results are encouraging it must be remembered that correlation (particularly at the levels shown in this work) at the best *suggests* causation and cannot prove the same. More experimental evidence is required to safely infer causation, which is the objective of our future work.

Using bivariate AR spectral estimation method, coherence analysis was performed between the EGG signal and finger PPG signal under fasting/postprandial conditions. The Vieira-Morf method was used for the computation of bivariate AR parameters. The results show that EGG and finger PPG are coherent at the GMA frequency (≈0.05 Hz) and level of coherence was between 0.5 and 0.7. In addition, the response delay in finger PPG induced by GMA is also implied in the negative coherence phase (see Figs. 8d and 9d). It has been shown that the level of coherence is sensitive to the GMA in this research.

The peripheral blood volume signal, measured by finger PPG, reflects the dynamics of the entire cardiovascular system. The measured volume is modulated by the heart and respiratory functions as well as by local mechanisms of resistance control. This study is limited to a small group of healthy volunteers and needs to be extended to larger groups and also include disease states. Results of this study primarily indicate a development of finger PPG technology in investigating the GI system. Extending this methodology to gastric pathology cases like stomach ulcer may provide further corroborative insights on finger PPG usage in the clinic, which can be undertaken as a future work.

In conclusion, obtaining GMA information in PPG signal might offer new insights into clinical diagnosis. The findings of this research show that the proposed method can detect GMA components among the lower frequencies of the finger PPG signal. Our future efforts will be directed toward actually reconstructing EGG from PPG. If this attempt results in success, we will have an elegant non-invasive clinical tool for monitoring gastric electrical activity in health and disease.

ACKNOWLEDGMENTS

We thank Applied Mechanics Department of Indian Institute of Technology Madras and Government of India for funding this work. We sincerely acknowledge all the volunteers who have participated in this study by sparing their valuable time and effort to make it successful. Authors would like to thank the unknown and anonymous reviewers for their invaluable comments to improve the standard of article.

REFERENCES

[1]Akaike, H. A new look at the statistical model identification. *IEEE Trans. Autom. Control* AC-19:716–723, 1974.
[2]Akay, M. Wavelet applications in medicine. *IEEE Spectr.* 34(5):50–56, 1997.
[3]Allen, J. Photoplethysmography and its application in clinical physiological measurement. *Physiol. Meas.* 28(3):R1–R39, 2007.
[4]Allen, J., and A. Murray. Similarity in bilateral photoplethysmographic peripheral pulse wave characteristics at the ears, thumbs and toes. *Physiol. Meas.* 21:369–377, 2000.
[5]Alos, R., E. Garcia-Granero, J. Calvete, and N. Uribe. The use of photoplethysmography to predict anastomotic viability after segmental intestinal ischemia in dogs. *Eur. J. Surg.* 159:35–41, 1993.
[6]Alvarez, W. C. The electrogastrogram and what it shows. *J. Am. Med. Assoc.* 78:116–119, 1922.
[7]Amara Grap. An introduction to wavelets. *IEEE Comput. Sci. Eng.* 2:2, 1995.
[8]Bendat, J. S., and A. G. Piersol. Engineering Applications of Correlation and Spectral Analysis (2nd ed.). New York: Wiley, 1993.
[9]Bendat, J., and A. Piersol. Random Data: Analysis and Measurement Procedures (3rd ed.). New York: Wiley, 2000.
[10]Brij, N. S., and K. T. Arvind. Optimal selection of wavelet basis function applied to ECG signal denoising. *Digit. Signal Process.* 16:275–287, 2006.
[11]Brillinger, D. Time Series: Data Analysis and Theory. New York: Holt, Rinehart and Winston, 1975.
[12]Cazares, S., M. Moulden, C. W. G. Redman, and L. Tarassenko. Tracking poles with an autoregressive model: a confidence index for the analysis of the intrapartum cardiotocogram. *Med. Eng. Phys.* 23:603–614, 2001.
[13]Challoner, A. V. J. Photoelectric plethysmography for estimating cutaneous blood flow. In: Non-Invasive Physiological Measurements, Vol. 1, edited by P. Rolfe. London: Academic Press, 1979, pp. 125–151.
[14]Chen, J., and R. W. McCallum. Response of the electric activity in the human stomach to water and a solid meal. *Med. Biol. Eng. Comput.* 29:351–357, 1991.
[15]Chen, J. D., W. R. Stewart, and R. W. McCallum. Spectral analysis of episodic rhythmic variations in the cutaneous electrogastrogram. *IEEE Trans. Biomed. Eng.* 40(2):128–135, 1993.
[16]Daubechies, I. The wavelet transform time-frequency localization and signal analysis. *IEEE Trans. Inf. Theory* 36(5):961–1005, 1990.
[17]Dean, C., E. D. Übeyli, and I. Cosic. Wavelet transform feature extraction from human PPG, ECG, and EEG signal responses to ELF PEMF exposures: a pilot study. *Digit. Signal Process.* 18:861–874, 2008.
[18]Dirgenali, F., S. Kara, and S. Okkesim. Estimation of wavelet and short-time Fourier transform sonograms of normal and diabetic subjects' electrogastrogram. *Comput. Biol. Med.* 36:1289–1302, 2006.
[19]Fleming, S. G., and L. Tarassenko. A comparison of signal processing techniques for the extraction of breathing rate from the photoplethysmogram. *Int. J. Biol. Med. Sci.* 2(4):232–236, 2007.
[20]Fujimura, J., M. Camilleri, P. A. Low, V. Novak, P. Novak, and T. L. Opfer-Gehrking. Effect of perturbations and a meal on superior mesenteric artery flow in patients with orthostatic hypotension. *J. Auton. Nerv. Syst.* 67:15–23, 1997.
[21]Garcia-Granero, E., S. A. Garcia, R. Alos, J. Calvete, B. Flor-Lorente, J. Willatt, and S. Lledo. Use of PPG to determine gastrointestinal perfusion pressure: an experimental Canine model. *Dig. Surg.* 20:222–228, 2003.
[22]Girault, J. M., D. Kouame, A. Ouahabi, and F. Patat. Microemboli detection: an ultrasound Doppler signal processing viewpoint. *IEEE Trans. Biomed. Eng.* 47:1431–1439, 2000.
[23]Guyton, A. C., and E. H. John. Textbook of Medical Physiology (11th ed.). Philadelphia: Elsevier/Saunders, 2006.
[24]Haghighi-Mood, A., and J. N. Tony. The-varying filtering of the first and second heart sounds. In: 18th Annual International Conference Proceedings of the IEEE EMBS Conference, Amsterdam, pp. 950–9516, 1996.
[25]Haghighi-Mood, A., and J. N. Tony. Coherence analysis of multichannel heart sound recording. In: IEEE Transactions on Computers in Cardiology, pp. 377–380, 1996.
[26]Halliday, D. M., J. R. Rosenberg, A. M. Amjad, P. Breeze, B. A. Conway, and S. F. Farmer. A framework for the analysis of mixed time series/point process data: theory and application to the study of physiological tremor, single motor unit discharges and electromyograms. *Prog. Biophys. Mol. Biol.* 64:237–278, 1995.
[27]Hertzman, A. B., and C. R. Spielman. Observations on the finger volume pulse recorded photoelectrically. *Am. J. Physiol.* 119:334–335, 1937.
[28]Hyndman, B. W., R. I. Kitney, and B. Sayers. Spontaneous rhythms in physiological control systems. *Nature* 233:339–341, 1971.
[29]Johansson, A., and P. A. Oberg. Estimation of respiratory volumes from the photoplethysmographic signal. Part 1: experimental results. *Med. Biol. Eng. Comput.* 37:42–47, 1999.
[30]Johansson, A., and P. A. Oberg. Estimation of respiratory volumes from the photoplethysmographic signal. Part 2: a model study. *Med. Biol. Eng. Comput.* 37:48–53, 1999.
[31]Jönsson, B., C. Laurent, M. Vegfors, and L. G. Lindberg. A new probe for ankle systolic pressure measurement using photoplethysmography. *Ann. Biomed. Eng.* 33:232–239, 2005.
[32]Kamal, A. A. R., J. B. Hatness, G. Irving, and A. J. Means. Skin photoplethysmography—a review. *Comput. Methods Programs Biomed* 28:257–269, 1989.
[33]Kara, S., F. Dirgenali, and S. Okkesim. Detection of gastric dysrhythmia using WT and ANN in diabetic gastroparesis patients. *Comput. Biol. Med.* 36:276–290, 2006.
[34]Kay, S. Modern Spectral Estimation. Englewood Cliffs, NJ: Prentice Hall, 1988.

[35]Kraitl, J., H. Ewald, and H. Gehring. Analysis of time series for non-invasive characterization of blood components and circulation patterns. *Nonlinear Anal. Hybrid Syst*. 2:441–455, 2008.
[36]Kvandal, P., S. A. Landsverk, A. Bernjak, U. Benko, A. Stefanovska, H. D. Kvernmo, and K. A. Kirkebøen. Low frequency oscillations of the laser Doppler perfusion signal in human skin. *Microvasc. Res*. 72(3):120–127, 2006.
[37]Kyriacou, P. A., A. Crerar-Gilber, R. M. Langford, and D. P. Jones. Electro-optical techniques for the investigation of photoplethysmographic signals in human abdominal organs. *J. Phys. Conf. Ser*. 45:232–238, 2006.
[38]Lee. J., and K. H. Chon. Respiratory rate extraction via an autoregressive model using the optimal parameter search criterion. *Ann. Biomed. Eng*. (in press). doi: 10.1007/s10439-010-0080-9.
[39]Liang, F., and H. Liu. A closed-loop lumped parameter computational model for human cardiovascular system. *JSME Int. J. C* 48:4, 2005.
[40]Lin, Z., and J. D. Chen. Time–frequency representation of the electrogastrogram—application of the exponential distribution. *IEEE Trans. Biomed. Eng*. 41:267–275, 1994.
[41]Lin, Y.-D., W.-T. Liu, C.-C. Tsai, and W.-H. Chen. Coherence analysis between respiration and PPG signal by bivariate AR model. *Conf. Proc. World Acad. Sci. Eng. Technol*. 53:847–852, 2009.
[42]Linkens, D. A., and S. P. Datardina. Estimation of frequencies of gastrointestinal electrical rhythms using autoregressive modeling. *Med. Biol. Eng. Comput*. 16:262–268, 1978.
[43]Marple, S. L. Digital Spectral Analysis with Applications. Englewood Cliffs: Prentice-Hall, 1987.
[44]Mizuno-Matsumoto, Y., S. Tamura, Y. Sato, R. A. Zoroofi, T. Yoshimine, A. Kato, M. Taniguchi, M. Takeda, T. Inouye, H. Tatsumi, S. Shimojo, and H. Miyahara. Propagating process of epileptiform discharges using wavelet-cross-correlation analysis in MEG. In: Recent Advances in Biomagnetism, edited by T. Yoshimoto. Sendai: Tohoku University Press, 1999, pp. 782–785.
[45]Nawap, S. H., and T. F. Quatieri. Short time Fourier transform. In: Advanced Topics in Signal Processing, edited by J. S. Lim, and A. V. Oppenheim. Englewood Cliffs, NJ: Prentice-Hall, 1988, pp. 239–337.
[46]Nilsson, L., A. Johansson, and S. Kalman. Monitoring of respiratory rate in postoperative care using a new photoplethysmographic technique. *J. Clin. Monit*. 16:309–315, 2000.
[47]Nitzan, M., S. Turivnenko, A. Milston, A. Babchenko, and Y. Mahler. Low-frequency variability in the blood volume pulse measured by photoplethysmography. *J. Biomed. Opt*. 1:223–229, 1996.
[48]Nitzan, M., A. Babchenko, B. Khanokh, and D. Landau. The variability of the photoplethysmographic signal: a potential method for the evaluation of the autonomic nervous system. *Physiol. Meas*. 19:93–102, 1998.
[49]Parkman, H. P. Electrogastrography: a document prepared by the gastric section of the American Motility Society Clinical Testing Task force. *Neurogastroenterol. Motil*. 15:89–102, 2003.
[50]Proakis, J. G., and D. G. Manolakis. Digital Signal Processing: Principles Algorithms and Applications (3rd ed.). India: Prentice-Hall, 1997.
[51]Roberts, V. C. Photoplethysmography—fundamental aspects of the optical properties of blood in motion. *Trans. Instrum. Meas. Control* 4:101–106, 1982.
[52]Rossi, P., G. I. Andriesse, P. L. Oey, G. H. Wieneke, J. M. M. Roelofs, and L. M. A. Akkermans. Stomach distension increases efferent muscle sympathetic nerve activity and blood pressure in healthy humans. *J. Neurol. Sci*. 161:148–155, 1998.
[53]Scalassara, P. R., C. D. Maciel, R. C. Guido, J. C. Pereira, E. S. Fonseca, A. N. Montagnoli, S. Barbon, Jr., L. S. Vieira, and F. L. Sanchez. Autoregressive decomposition and pole tracking applied to vocal fold nodule signals. *Pattern Recognit. Lett*. 28:1360–1367, 2007.
[54]Semmlow, J. L. Biosignal and Medical Image Processing (2nd ed.). Boca Rotan: CRC Press, 2009.
[55]Smout, A. J., E. J. Van der Schee, and J. L. Grashuis. What is measured in electrogastrography? *Dig. Dis. Sci*. 25:179–187, 1980.
[56]Stefanovska, A., M. Bračič, and H. D. Kvernmo. Wavelet analysis of oscillations in the peripheral blood circulation measured by laser Doppler technique. *IEEE Trans. Biomed. Eng*. 46(10):1230–1239, 1999.
[57]Texter, E. C. Small intestinal blood flow. *Dig. Dis. Sci*. 8(7):587–613, 1963.
[58]Thomas, K. A., M. Moosikasuwan, D. S. Samir, and S. D. Kedar. Length-normalized pulse photoplethysmography: a noninvasive method to measure blood hemoglobin. *Ann. Biomed. Eng*. 30:1291–1298, 2002.
[59]Übeyli, E. D., D. Cvetkovic, and I. Cosic. AR spectral analysis technique for human PPG, ECG and EEG signals. *J. Med. Syst*. 32(3):201–206, 2008.
[60]Unser, M., and A. Aldroubi. A review of wavelets in biomedical applications. *Proc. IEEE* 84(4):626–638, 1996.
[61]Wukitsch, M. W., M. T. Petterson, D. R. Tobler, and J. A. Pologe. Pulse oximetry: analysis of theory, technology and practice. *J. Clin. Monit*. 4:290–301, 1988.